



Original Article

Semi-solid process of 2024 wrought aluminum alloy by strain induced melt activation

Surachai Numsarapatnuk^{1*} and Sukangkana Chayong²

¹ *Department of Industrial Engineering, Faculty of Engineering, Ubon Ratchathani University, Warin Chamrap, Ubon Ratchathani, 34190 Thailand.*

² *Department of Industrial Engineering, Faculty of Engineering, Khon Kaen University, Mueang, Khon Kaen, 40002 Thailand.*

Received 16 November 2012; Accepted 1 July 2013

Abstract

The aim of this study is to develop a production process of a fine globular structure feedstock of the 2024 aluminum alloy suitable for subsequent semi-solid forming. The 2024 wrought aluminum alloy was first annealed to reduce the effect of work hardening. Then, strain was induced in the alloy by cold compression. After that the microstructural evolution during partial melting was investigated. The samples were subjected to full annealing at 415°C for 3 hrs prior to cold compression of 40% reduction of area (RA) with 3 mm/min strain rate. After that samples were partially melted at 620°C with varying holding time from 0 to 60 min followed by water quenching. The grain size and the average grain diameter of solid grains were measured using the linear intercept method. The globularization was interpreted in terms of shape factor. Liquid fraction and the distribution of the eutectic liquid was also investigated. It was found that during partial melting, the globular morphology was formed by the liquid wetting and fragmentation of high angle boundaries of recrystallized grains. The suitable semi-solid microstructure was obtained from a condition of full annealing, 40% cold working and partial melting at 620°C for 6 min holding time. The near globular grains obtained in the range of 0-60 min consisted of uniform spheroid grains with an average grain diameter ranged from 73 to 121 μm, quenched liquid fraction was approximately 13–27% and the shape factor was greater than 0.6. At a holding time of less than 6 min, grain coarsening was dominant by the immigration of high-angle grain boundaries. At a longer holding time, liquid fraction increased and Ostwald ripening was dominant. The coarsening rate constant for the 2024 Al alloy was 400.36 mm³.s⁻¹. At a soaking time of 60 min, it was found that a minimum diameter difference was 1.06% with coarsening index n=3 in a power law equation. The non-dendritic slug of 2024 alloy was rapidly compressed into a disc with 90%RA and exhibited uniform structure.

Keywords: Al2024, semi-solid, SIMA process, globular microstructure

1. Introduction

In general, conventional metal shaping process has been carried out in a solid state as a starting feedstock through a hot or cold working, such as extrusion, forging, rolling and machining. Metal used in this type of forming is a

group of wrought metal alloy, whereas fully liquid metal with high temperature is shaped in a mould in a casting process. Semi-solid metal (SSM) casting is a novel technology for forming metals, which is different from both conventional processes because it forms the metal in to the die in a solid-liquid state at a temperature within the liquidus and solidus temperature. Such semi-solid slurry favor consists of fine globular solid grains suspended in liquid metal. This process can be applied to both wrought and cast metal alloys. Before forming, semi-solid slurry is either agitated or sheared by an

* Corresponding author.

Email address: surachai_n@hotmail.com

appropriate method in order to be able to transform into a fine globular solid with 30-50% liquid fraction uniformly distributed in liquid matrix (Atkinson *et al.*, 2003; Liu *et al.*, 2003). The slurry with 30-50% liquid has thixotropic properties, meaning when stirred or sheared the viscosity decreases and when it is left standing, its viscosity recovers to the original state again (Chayong *et al.*, 2005). Advantages of the SSM process are: 1) a complex geometrical product with a thin wall can be formed with less air entrapment and shrinkage porosities, 2) a longer die life, and 3) energy savings compared to other methods. The SSM casting is classified into two key processes, rheocasting and thixoforming. Rheocasting is a liquid metal stirred during cooling into a semi-solid region to become non-dendritic followed by casting into a component directly without an intermediate step of feedstock solidification. Thixoforming consists of three major steps: firstly, the production of feedstock with a fine globular structure, then reheating it into semi-solid state using electric induction furnace, and finally, the slurry are shaped in the die into a near net shape part. If the slurry is injected into a closed die with high pressure, this is called thixocasting. If it is with a lower liquid fraction of around 30-40%, a semi-solid slug is forged using an upper and a lower die into a part, such as an automobile part, this is refer to as thixoforging. Another process using a feedstock in form of a solid state instead different from previous mentioned processes is thermomechanical treatment as stress induced melt activation (SIMA) and RAP (recrystallized and partial melting). Moreover, a particular SSM process for magnesium alloy is a thixomoulding; the SSM process of forming a fiber-reinforced metal matrix composite (MMCs) is a compocasting.

SIMA process was developed by D.H Kirkwood and colleagues at the University of Sheffield in England (de Figueredo *et al.*, 2001). The direct chill casting feedstock with a dendritic structure was hot extruded over the recrystallization temperature. It was moderately or severely cold deformed to induce sufficiently internal residue plastic strain and then reheated to high temperature (Kirkwood *et al.*, 1994). During reheating in solid state, there is a series of processes called recovery, recrystallization, and grain growth. The driving force for these processes is derived from the residue strain energy. When the temperature rises into semi-solid range and the alloy is held for appropriate time, liquid content increased. Then, liquid penetration occurred and wetting along the solid grains boundaries and finally, liquid melting the solid grains become globular. Semi-solid slurry is then cast into a feedstock suitable for thixoforming. The advantage

of feedstock produced by SIMA as compared with other SSM processes using liquid metal such as MHD stirring (a popular method), cooling slope (CS), low superheat casting, GISS with gas spraying, and others, is that globular structure consists of the finer, more uniform and globular grains (Fan *et al.*, 2002). It is convenient because most of supplied wrought Al alloys have already been plastically deformed. These problems limit the capacity of SIMA process in commercial applications as follows (Fan *et al.*, 2002): 1) High cost of feedstock and a small number of its suppliers. 2) Usually limited to feedstock of diameters smaller than 37 mm, because larger ones have inhomogeneous microstructure. 3) A more suitable process knowledge from a large number of research work is required.

Therefore, the aims of this work are to study the suitable method in producing a semi-solid feedstock from Al 2024-T4 wrought alloy by applying modified SIMA technique. The 2024 Aluminum alloy is a wrought specification AlCu system. The alloy requires full annealing to reduced work hardening and precipitation hardening effects, which ease for subsequent cold working. The strain induced stage will be carried out using compression instead of extrusion to produce uniform deformed grain. The amount of cold compression must be greater than a critical deformation to ensure a sufficient amount of an internal driving force for recrystallization during partial remelting. Suitable semi-solid temperature range and appropriate liquid fraction were studied. The coarsening kinetics of primary α (Al) globular structure was also studied.

2. Experimental

The experiment was performed using the commercially extruded AA 2024-T4 (Al-4Cu-Mg) rods supplied by Thyssen Krupp Materials (Thailand) Company Limited, in a form of 80 mm in diameter. However, the extrusion ration was not available from the supplier. The chemical composition of 2024 alloy is shown in Table 1. The Aluminum Association Standard (AA) is also shown as a comparison. Figure 1 is a cooling curve of the 2024 alloy measured using K type thermocouple from molten aluminum alloy with the cooling rate of 0.44°C/s (or 4.2°C/min). The solidus temperature (T_s) and the liquidus temperature (T_L) were approximately 490°C and 640°C, respectively.

The reheating slugs were machined into small cylinders of 30 mm in diameter and 75 mm long. The reheating process was consists of three steps as shown in Figure 2. In the first step, the slug was fully annealed at 415°C at a

Table 1. Chemical composition of as received 2024 wrought aluminum alloy.

Material	Cu	Mg	Mn	Fe	Si	Zn	Ti	Cr	Ni	Pb % wt
As received	4.368	1.503	0.641	0.238	0.222	0.23	0.009	0.008	0.003	0.007
Standard	3.8-4.9	1.2-1.8	0.3-0.9	<0.5	<0.5	<0.25	<0.15	<0.1	<0.05	<0.05

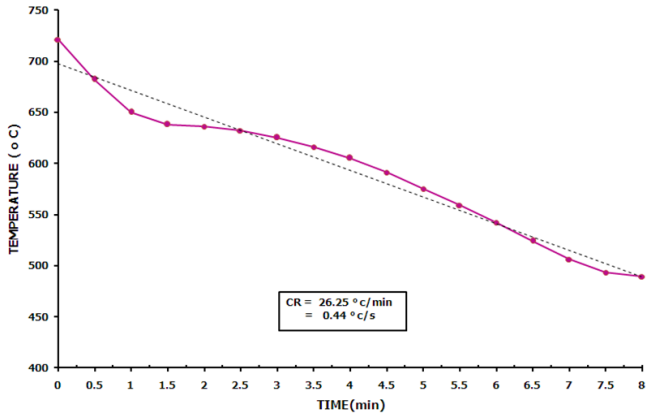


Figure 1. Cooling curve of 2024 wrought aluminum alloy measured in this work.

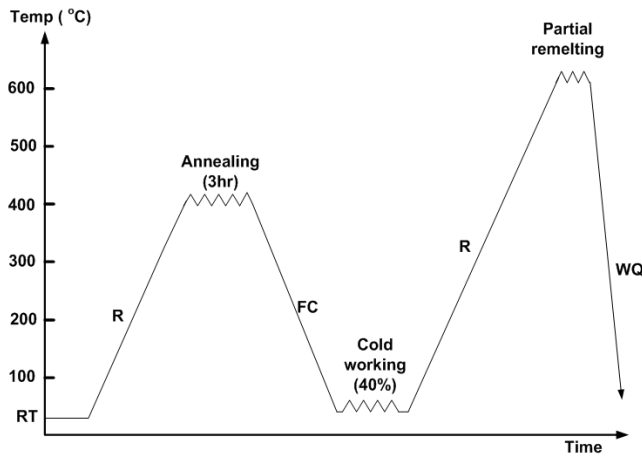


Figure 2. Schematic diagram of the stages of SIMA process used in this experiment.

heating rate of 4.2°C/min for 3 hrs, partially melted in an induction furnace at temperature 620°C – associated with 55% liquid fraction as suggested by Backerud *et al.* (1986) – and finally slowly cooled to room temperature in the furnace as shown in Figure 3.

In the second stage, annealed specimens were cut into cylinders of Ø 30 mm × 45 mm for cold working. Specimens were compressed with a strain rate of 3 mm/min to 40% RA using a 200 ton hydraulic press. The stress–strain relationship is plotted in Figure 4. The percent reduction of area (% RA) is a function of a reduction of height ($h_o - h_f$), therefore it can be computed by Equation 1, where h_o and h_f are the height of sample before and after compression, respectively.

$$\%RA = \frac{(h_o - h_f)}{h_f} \times 100 \quad (1)$$

In the final stage, all specimens were then heated to semi-solid temperature of 620°C and held for 0, 1, 2, 3, 4, 5, 6, 10, 20, 30, and 60 minutes. After that all specimens were quenched in water.

Microstructures of the quenched samples were investigated at various positions on a quarter of a cross section area, as shown in Figure 5. Specimens were mechanically polished and etched with Keller’s etchant (1 ml HF + 1.5 ml HCl + 2.5 ml HNO₃ + 99.5 ml H₂O). The recrystallized grain size, fraction of quenched liquid (f_L), and shape factor (SF) were measured from micrographs using an image analysis software called Olysia m3. Hardness test of all samples were carried out using the Rockwell hardness test.

A rapid compression trial was performed by compressed semi-solid slug into a disc. This trial test was performed to investigate the thixoformability and its micro-

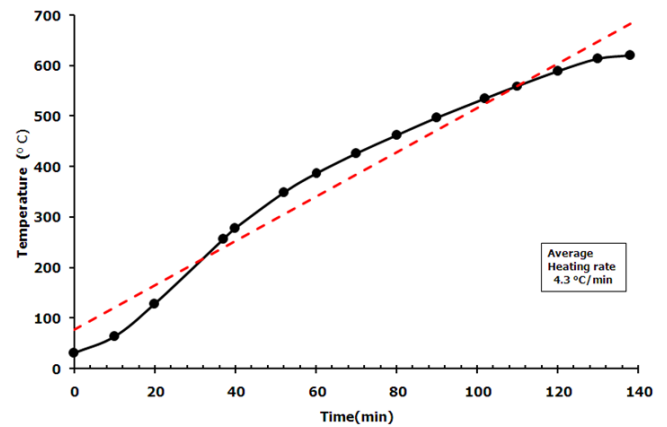


Figure 3. The reheating curve of compressed 2024 slugs.

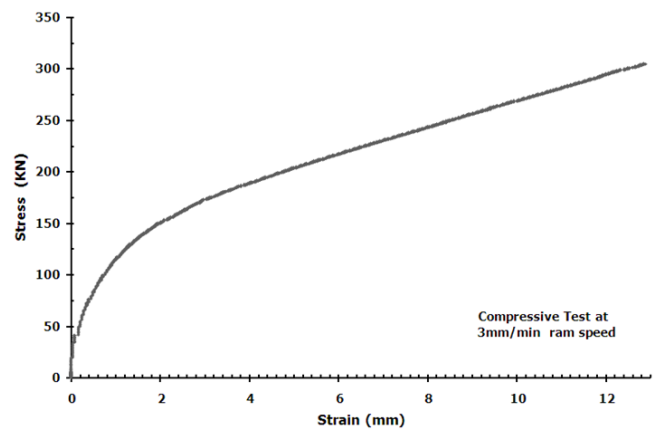


Figure 4. Stress–strain curve obtained from the compression test.

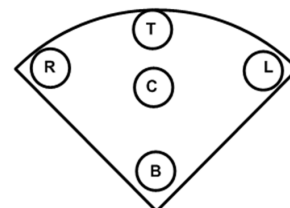


Figure 5. Positions for micrographs on a quarter of cross section area of samples.

structure of the feedstock. The feedstock with dimension of $\varnothing 86 \times 86$ mm, was full annealed, with cold compression and remelting. After 6 min holding at 620°C , the slug was compressed at a speed of 50 mm/s.

3. Results and Discussion

3.1 Effect of annealing

In Figure 6(a) the microstructure in longitudinal section of the received sample consisted of an elongated grains or fibrous structure with high quantity of intermetallic particles along an extruded direction. Hardness of Al2024-T4 was 81.75 HRB (equivalent to 160 HV). During full annealing at 415°C for 3 hrs, there were continuous processes: recovery, recrystallization, and grain growth causing the deformed structure transformed into the equiaxed grained structure. Most second-phase particles in colored bands have resolved back to a-solid solution phase as the sample was being soaked at annealing temperature. During slow cooling, these particles such as Al_2CuMg (S phase) Al_2Cu , Mg_2Si , and others (Fujda *et al.*, 2007) precipitate out, coagulate and uniformly distributed throughout the a matrix phase again. These second-phase particles inhibit the growth of recrystallized grains as well indicated in Figure 6(b). After full annealing, hardness decreased due to recrystallization. The average hardness of annealed sample was 23 HRB. Therefore, the annealed 2024 alloy has low strain hardening and low stored strain energy derived from the previous deformation (Smith, W.F. *et al.*, 1990).

3.2 Effect of cold working

The annealed 2024 alloy was plastically deformed at 40% RA which was higher than the amount of the critical deformation which is usually 2-20% RA (Callister *et al.*, 2000). The compression performed with a ram speed of 3 mm/min to ensure sufficient stored strain energy in the alloy, which will be later served as a driving force for recover and recrystallization process and internal strain distributed on the deformed structure. The average hardness of cold worked samples was 33 HRB. Due to cold working, dislocation density increased (the number of dislocations increased by multiplication processes). Work hardening effect led to an increase of the hardness and strength because the external applied stress must be greater than the internal stress in order to move a dislocation through other dislocations and/or obstruct in the crystal structure. For this reason, the grain morphology remained as the elongated grained structure after working. The sufficient shear stress causes individual grains to slip and twin, afterwards, the entire grains are distorted, constrained to some degrees, extended in the rolling direction perpendicular to a force direction as shown in Figure 6(c). Although most of the mechanical energy obtained from the previously cold working has been partially transformed into heat, the residual strain energy around

5-6% has been still accumulated in crystal structure of the alloy (Callister *et al.*, 2000). When the alloy was heated in the partial remelting stage, this stored internal energy was supplied as the driving force to promote fully recovery and recrystallization process during heating in solid state.

3.3 Liquid fraction during partial melting

The annealed 2024 Al alloy after 40% RA compression was heated to 620°C to generate 55% fraction liquid according to Backerud *et al.* (1986). From Figure 7, quenched liquid fraction measured from micrographs showed only about 13 to 27% of liquid, which is less than the amount suggested by Backerud *et al.* (1986). This may caused by several factors as following: (1) The method used to determine the liquid fraction was different. In this experiment it was measured from quenched samples while Backerud *et al.* (1986) measured the amount of liquid during slow cooling of $0.8^\circ\text{C}/\text{s}$. (2) Slow cooling rate during transferring the sample from the furnace to a water tank. Some amount of liquid might have been solidified to solid phase or compounds. (3) Heat sensitivity of the wrought alloy means that the temperature of the sample slightly changes in semi-solid temperature range causing the liquid quantity significantly to change; thus, the temperature of the sample inside the furnace must be precisely controlled. Finally, (4) liquid segregations and tiny liquid droplets were formed inside semi-solid grains causing difficulties in the measurement.

3.4 Effect of holding time on microstructure during partial melting

The microstructural evolution of 2024-T4 alloy after full annealing, 40% RA cold compression and partial melting with holding time of up to 60 min is shown in Figure 8.

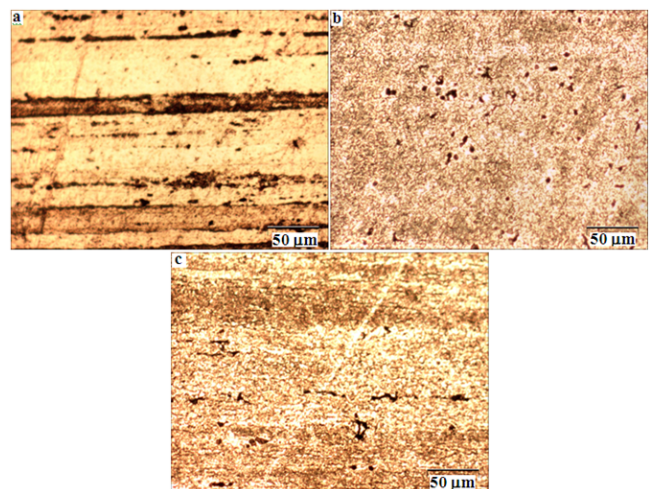


Figure 6. Microstructures of 2024 Al alloy in longitudinal direction: (a) as received (b) full annealed, and (c) 40 % RA cold worked.

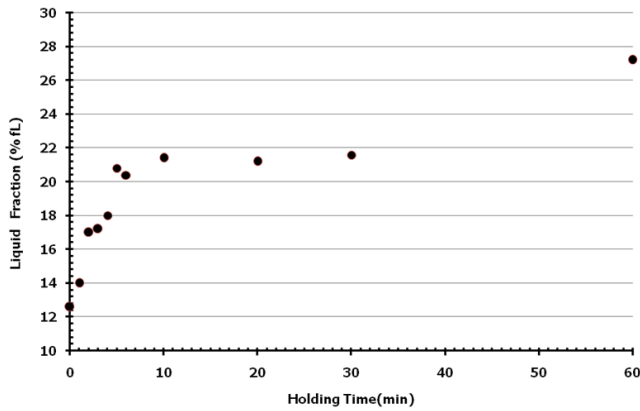


Figure 7. Quenched liquid fraction (f_L) against holding time (t) in the range 0-60 min at semi-solid temperature 620°C obtained from quenched samples. NOTE: this figure has no reference in the text.

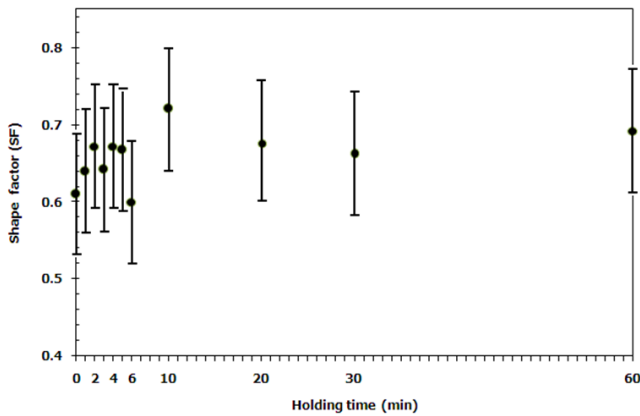


Figure 8. Shape factor (SF) of solid grains of quenched specimens that held at 620°C for various holding time.

The partially melt specimens exhibited shape factor (SF) values more than 0.6 in all conditions (SF=1 means a perfectly circle morphology). The result of microstructural investigation at various holding times is shown in Figure 9 and 10. In Figure 9, the grain size increased with increasing holding time. At short holding times up of to 5 minutes, the average grain diameter (d) increases gradually from around 73 mm to 82 mm as shown in Figure 9(a) to (f), and after that at a holding time of 6, 10, 20, 30 and 60 min, the grain size steadily increased to 88, 92, 94, 105, 121 mm, respectively. The liquid phase along grain boundaries increases continuously to become a thick liquid film. In addition, there were also some tiny liquid pools entrapped in solid grains. The amount of entrapped liquid decreased with increasing holding time.

The mechanism of microstructural evolution taken place during heating can be described as following. Recovery occurred when the dislocation density decreased; atoms rearrange themselves to form new subgrains and a reduction of stored energy in the metal. Then, the recrystallization took place at higher temperature ranges to form a new equiaxed

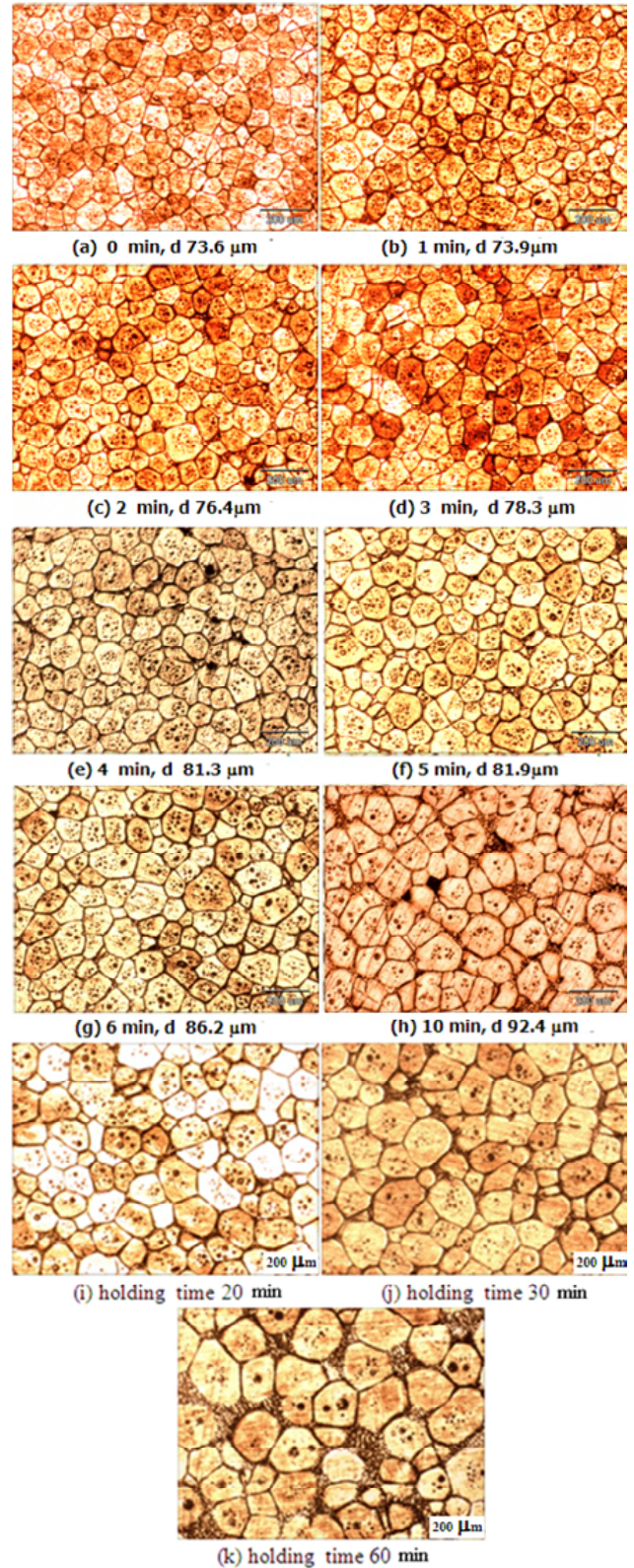


Figure 9. Microstructural evolution of quenched samples at position C after 40 % RA, partial remelting at 620°C for 0-10 min holding time. The average grain sizes are the following: (a) 73.6 μm , (b) 73.9 μm , (c) 76.4 μm , (d) 78.3 μm , (e) 81.3 μm , (f) 81.9 μm , (g) 88.2 μm , and (h) 92.4 μm , (i) 94.3 μm , (j) 105.3 μm , and (k) 121.3 μm .

grained structure with a free strain instead of the cold deformed metal structure (Smith, 1990). Finally, the grain growth then continually coarsened of these recrystallized grains by a mechanism of motion of high angle grain boundaries; the angle between the crystallographic orientation of a grain and that of a connected grain is more than 20° (Chayong *et al.*, 2002). In addition, there is an atomic motion by short diffusion in the direction opposite to the direction of the boundary motion from one grain across a boundary to an adjacent grain in order to decrease the total boundary area energy (γ_B) and which is resulting in an increase of the grain size but a decrease in the number of grains. All previously mentioned processes took place below a solidus temperature in a solid state. When the temperature goes beyond the solidus temperature (about 490°C), up to the required temperature of 620°C , a liquid phase initially forms along the recrystallized grain boundaries containing a segregation of solute elements, impurities, and other phases, which have the lowest melting point. With a longer holding time, the amount of eutectic liquid gradually increases around the solid grains, then dissolves or wets new grain boundaries and breaks them down as fragments of dendritic arms; because the free energy of high angle boundary (γ_{GB}) is greater than twice the energy of the solid-liquid interface ($2\gamma_{SL}$) (Atkinson *et al.*, 2008). Therefore, these semi-solid polygon grains have been accommodated and become near globular grains; simultaneously, grains still continue to grow to an appropriate and homogeneous sizes (less than $100\ \mu\text{m}$), and a larger liquid quantity depends on time (Liu *et al.*, 2003).

If there were excessive holding times, the slurry containing coarse grain structure will be difficult to flow during the forming, and the products will have poor mechanical properties. From Figure 10 it can be seen that the microstructures at various positions on the same cross sectional sample without holding time were entirely fine equiaxed grains with little liquid phase. It can further be seen that during heating, the driving force from cold working was sufficient to induce recrystallization completely and sufficient time favors the growth of grains at a low heating rate ($4.3^\circ\text{C}/\text{min}$). When the temperature rises over the solidus line to semi solid 620°C without holding, the sample was then immediately water-quenched. Therefore, there was a small amount of liquid discontinuously penetrated along the boundaries with an average solid grain size (d) of $\sim 74\ \mu\text{m}$ and 12.6% liquid fraction. The characteristics of semi-solid microstructures at all locations in all samples, which were held in the range of 0-60 min, appeared to near globular grain structure with uniform in size, and their globularization is more than 0.6 at all conditions. However, slightly liquid segregation has been observed but the difference of liquid fraction in each position was less than 10%. For example, in Figure 11 they were entirely globular microstructures (C, B, T, L, R) after 6 min of holding time. The α globular diameter (d) was $88\ \mu\text{m}$, the shape factor (SF) was 0.61 and the distribution of quenched liquid fraction (f_L) was between 17% and 22% with a difference of 5%.

3.5 Grain coarsening mechanism during partial melting

The partial melting process may be divided into three stages: fragmentation, globularization, and grain coarsening previously mentioned (Chayong *et al.*, 2002). The coarsening mechanism is possible as two models that are the migration of high angle grain boundaries (smaller grains are absorbed by larger ones) and the Ostwald ripening describing here as following: It is a spontaneous process where smaller grains have a higher ratio of surface area to volume yielding higher surface energy than that larger ones. Therefore, atoms on surfaces of smaller grains, are less stable, tend to continually detach out and diffuse into eutectic liquid surrounding them following the Kelvin equation. With longer time, the concentration of free atoms in the liquid gradually increases until the liquid becomes a supersaturated solution. Thus, these atoms must be transferred to the liquid of lower concentration around larger grains and redeposited on their surfaces. As a result, the number of smaller grains continues to shrink and disappear; meanwhile, larger grains continue to grow and

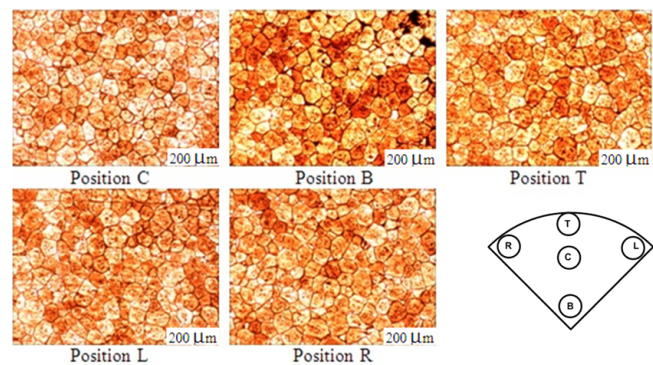


Figure 10. Globular microstructures at various positions on a quarter of cross section area of the quenched sample after annealing, 40% RA, partial melting at 620°C without holding time.

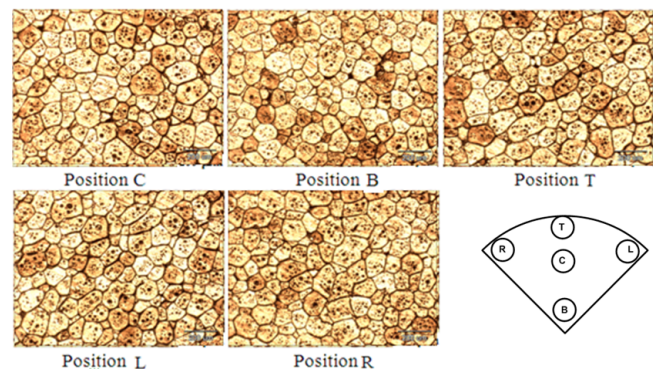


Figure 11. Globular microstructures at various positions on a quarter of cross section area of quenched sample after annealing, 40% RA and partial reheated at 620°C for 6 min.

modify as globule grains, which reduces the surface area for the minimum surface energy (Bolouri *et al.*, 2010). The study of coarsening (growth) of solid grains in semi-solid slurry can be explained by the Lifshitz-Slyozov-Wagner (LSW) theory, where the average grain diameter (d) with exponential n is a function of holding time (t) following a power law as shown in Equation 5.

$$\bar{d}^n - \bar{d}_0^n = k.t \quad (5)$$

where \bar{d} and \bar{d}_0 are the average grain diameter at time t and $t=0$, k is the coarsening rate constant, t is holding time, and n is the coarsening index. The coarsening index is $n=2$ if the grain coarsening is controlled by grain boundary motion or by an interface reaction mechanism. $n=3$ is for the Ostwald ripening or by volume diffusion, and $n=4$ for boundary diffusion (Bolouri *et al.*, 2010). Tzimas and Zavaliangos (2000) studied the coarsening of globular microstructure in semi-solid alloy produced by SIMA and by magnetohydrodynamic (MHD) stirring. They proposed that as soon as the liquid was formed at grain boundaries, Oswald ripening and the motion of grain boundary kinetics were thought to carry out simultaneously and independently. Bolouri *et al.* (2010) observed that a boundary between two connected solid grains disappears to become a single large gain with a neck rather than a globular grain and it tends to be often found in initial time of partial melting stage. This phenomenon means that the growth of solid grains is easily formed by atomic diffusion across the boundaries in the mechanism of high angle grain immigration. It can be seen in Figure 9 that the numbers of necks decreasing, whereas in contrast the number of fine broken dendritic arms suspended in the liquid film at those grain boundaries increased and were distributed non-uniformly, clearly seen in Figure 9(k). This implies that grain coarsening was driven by both kinetics simultaneously but at different rate. At short holding times of less than 6 min, the grain boundary immigration plays a key role because a large number of solid grains were connected tightly. Therefore, a larger number of atoms can easily diffuse from smaller grains through solid boundaries to larger ones. In case of longer holding time of more than 6 to 60 min with high liquid fraction, most of solid grains were connected with soaked liquid boundaries instead. This phenomenon increases the opportunity for coarsening by Ostwald ripening kinetics or liquid boundary immigration. Comparing the graphs plotted from power law of Equation 5 with given $n=1$, $n=2$, and $n=3$ as expressed in Figure 12–14, the grain size increased with an increase in holding time. The R^2 of the graph with $n=3$ shows the highest value, close to 1. This indicates that the graph in Figure 14 can be used for the prediction of d^3 due to the coefficient of determination of d^3 was 96.9% and the coarsening rate (k) measured from the slope of this graph is $400.36 \mu\text{m}^3 \cdot \text{s}^{-1}$. Atkinson *et al.* (2010) pointed out that a high value of $k > 600 \mu\text{m}^3/\text{s}$ can be obtained from casting Al alloy and a low value of $k < 600 \mu\text{m}^3/\text{s}$ can be obtained in wrought Al alloy. In addition, the value of k also depends on the production technique of globular microstructure for example; SIMA,

RAP, CS (cooling slope) GISS, and others, and a variation in the composition of the alloy. The grain size (d) at 60 min holding time was calculated from Equation 5 with $n=1$, $n=2$,

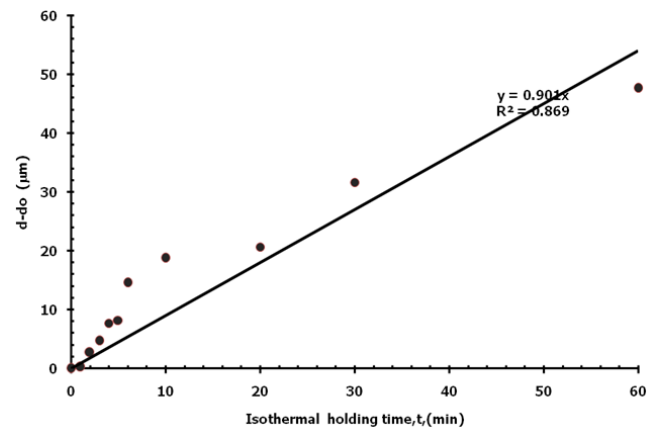


Figure 12. Grain size (d) and holding time (t) within 60 minutes at 620°C .

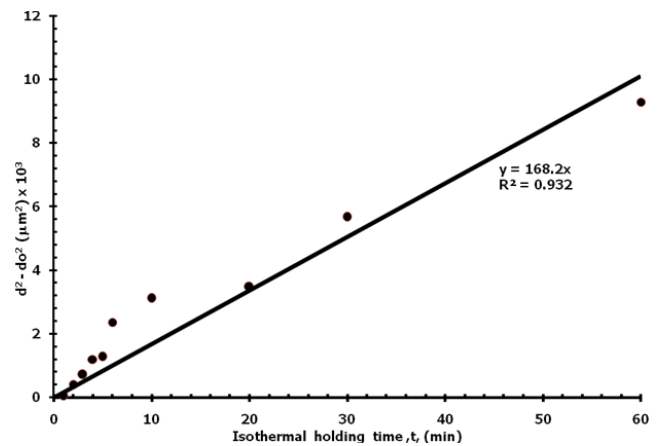


Figure 13. Square grain size (d^2) and holding time (t) within 60 min at 620°C .

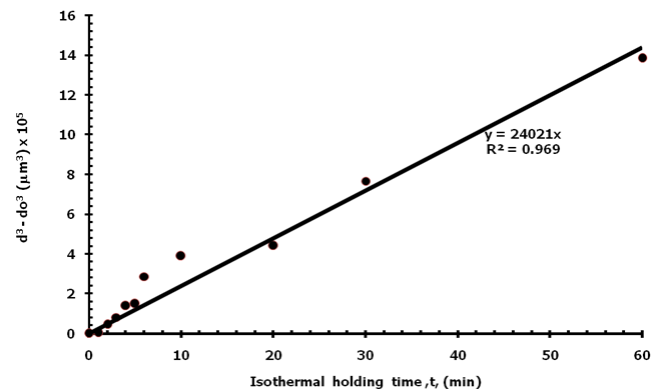


Figure 14. Cubic grain size (d^3) and holding time (t) within 60 min at 620°C .

and $n=3$ to in order to compare it with the grain size measured from the experiment, which was equal to $121.3 \mu\text{m}$. The difference of grain diameter (Δd) for $n=1$, $n=2$ and $n=3$ were 5.26%, 2.72%, and 1.06%, respectively. The difference was lowest for $n=3$, thus, the grain coarsening could be mostly controlled by Oswald ripening.

When the holding time increased, the number of tiny droplets decreased with an increase of the amount of large droplets and they become rounder. Fan *et al.* (2002) proposed that during solidification in semi-solid state, initially the coalescence of dendrite arms was very rapid; if they have preferential crystallographic orientation yielding small amounts of liquid entrapped in an inter-dendritic region to become tiny droplets inside the grain later. There are two possible models of droplet coarsening. Liquid boundary immigration is the coalescence of two tiny adjacent droplets into a larger one and Ostward ripening, where an unstable droplet is transported to agglomerate with another far away one or with liquid boundaries. These actions occur in order to reduce the total area of the solid-liquid interface in its system (Bolouri *et al.* 2010).

Figure 15 shows microstructures across the centerline of thixoformed slug. The pressed sample exhibited uniform non-dendritic structures. However, the sample was cracked as soon as compressed. This implies that the speed of forming was too slow and there was a small amount of liquid, therefore, semi-solid slurry was cooled prior forming. The hardness of the thixoformed sample was 63 HRB. However, hardness can be increased by heat treatment.

4. Conclusions

Following conclusion can be drawn from the results of this study:

1. The 2024 wrought aluminum alloy, through full annealing plus SIMA, exhibited a near globular structure with a shape factor of more than 0.6 in all conditions. These ensure flow ability and final product properties.

2. The optimal globular microstructure obtained by this novel SIMA route include three steps; full annealing at 415°C for 3 hrs, cold compression at around 40% RA with constant strain rate of $3 \text{ mm}\cdot\text{min}^{-1}$ and partial remelting at 620°C for 6 min. The globular structure contains α solid grains with uniform grain size and with average grain diameter of $88.2 \mu\text{m}$ surrounded by an eutectic liquid of about 27% quenched liquid.

3. The mechanism of α -Al globular grain coarsening in short holding time around ≤ 6 min was immigration of high angle grain boundaries. At longer periods > 6 to 60 min the Oswald ripening is dominant. The coarsening rate constant (k) of 2024 wrought aluminum alloy through full annealing plus cold compression method was approximately $404.0 \mu\text{m}^3\cdot\text{s}^{-1}$.

4. The temperature control and rapid forming speed are important parameter to ensure thixoformability of the non-dendritic slug.

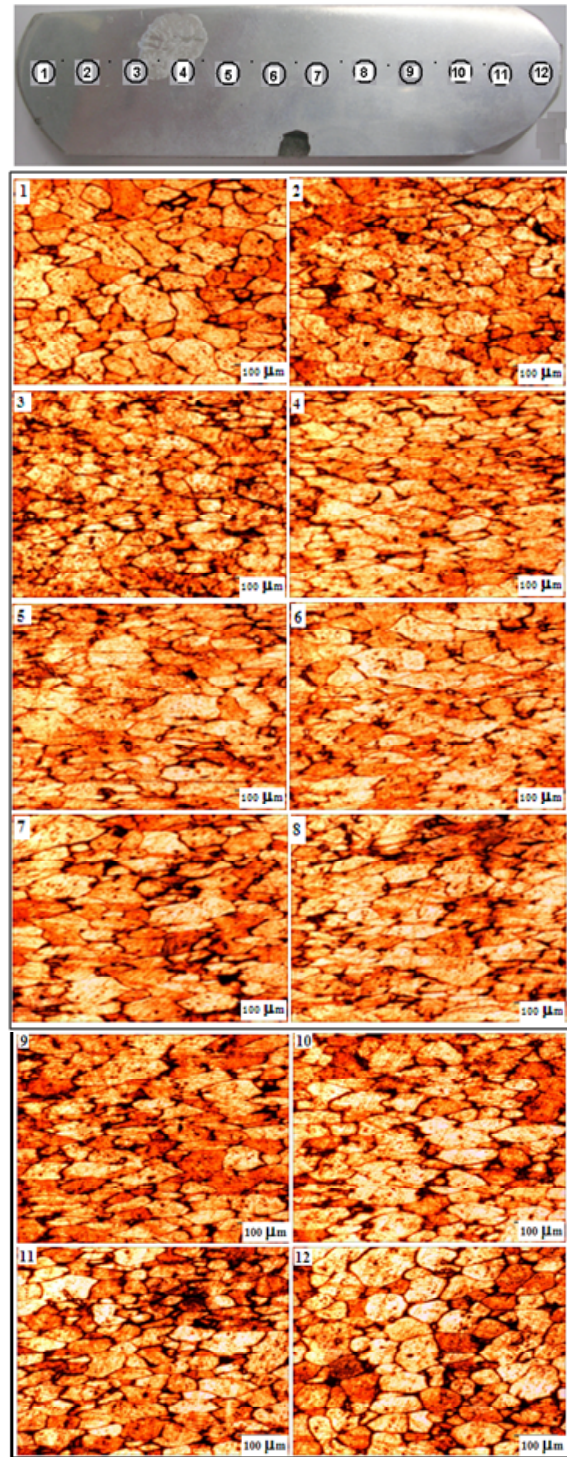


Figure 15. Microstructures across the centered line of the thixoformed slug with 91% RA.

Acknowledgment

The authors would like to thank to Department of Industrial Engineering, Faculty of Engineering, Ubon Rachathani University for research fund and experimental facilities, and S. Chayong for fruitful comments.

References

- Atkinson, H.V. and Liu, D. 2010. Coarsening rate of microstructure in semi-solid aluminium alloys. *Transactions of Nonferrous Metals Society of China*. 20, 1672–1676.
- Atkinson, H.V., Burke, K. and Vaneetveld, G. 2008. Recrystallisation in the semi-solid state in 7075 aluminium alloy. *Materials Science and Engineering A*. 1(1), 973-976.
- Backerud, L., Krol, E. and Tamminen, J. 1986. Solidification characteristics of aluminium alloy: Wrought alloys, Skanuminium, Universitetsforlaget AS, Oslo, Norway.
- Bolouri, A., Shahmiri, M. and Cheshmeh, E.N.H. 2010. Microstructural evolution during semi-solid strain induced melt activation process of aluminum 7075 alloy. *Transactions of Nonferrous Metals Society of China*. 20, 1663-1671.
- Callister, Jr. and William, D. 2000. *Materials Science and Engineering: An Introduction* (5th edition), John Wiley & Sons, Inc., U.S.A.
- Chayong, S. 2002. Thixoforming Processing of Aluminium 7075 Alloy, Department of Engineering Materials, The University of Sheffield, England.
- Chayong, S., Atkinson, H.V. and Kapranos, P. 2005. Thixoforming 7075 aluminium alloy. *Materials Science and Engineering A*. 390, 3–12.
- de Figueredo, A. 2001. Science and technology of semi-solid metal processing, North American Die Casting Association, Rosemont, Illinois, U.S.A.
- Fan, Z. 2002. Semisolid metal processing. *International Materials Reviews*. 47(2), 1-37.
- Fujda, M., Misicko, R., Rusnakova, L. and Sojko, M. 2007. Effect of solution annealing temperature on structure and mechanical properties of EN AW 2024 aluminum alloy. *Journal of Metal Materials and Minerals*. 17(1), 35-40.
- Kirkwood, D.H. 1994. Semisolid metal processing. *International Materials Reviews*. 39(5), 173.
- Liu, D., Atkinson, H.V., Kapranos, P., Jiratticharoan, W. and Jones, H. 2003. Microstructure evolution and tensile mechanical properties of thixoformed high performance aluminium alloys. *Materials Science and Engineering A*. 361, 213-224.
- Smith, W.F. 1990. *Material Science and Engineering* (2nd edition), McGraw-Hill, U.S.A.
- Tzimas, E. and Zavaliangos, A. 2000. Evaluation of volume fraction of solid in alloy formed by semi solid processing. *Journal of Materials Science*. 35, 5319-5329.